Progress In Electromagnetics Research M, Vol. 64, 201–209, 2018

A Compact Tri-Band Bandpass Filter Using Two Stub-Loaded Dual Mode Resonators

MuhibUr Rahman and Jung-Dong Park*

Abstract—In this paper, we present a compact tri-band bandpass filter (BPF) using two stub-loaded dual mode resonators (SLDMRs) combined with intra-coupled internal resonators. The designed filter operates at 1.575, 2.4, and 3.45 GHz, corresponding to the GNSS, WLAN, and WiMAX applications, respectively. The passbands of the filter are determined by odd- and even-mode frequencies created by the SLDMR and the internal open loop resonator inside of it. The corresponding even-mode frequency can be adequately tuned by adjusting the length of the stub while the odd-mode frequency is fixed. Two transmission zeros (TZ's) are introduced on each side of the passband to improve the selectivity of the implemented filter. Five TZ's around the edges of three passbands make the passbands highly isolated, and these TZ's can be placed according to the desired choice. The proposed tri-band BPF was designed, fabricated and measured, and the simulated and measured results corresponded very well.

1. INTRODUCTION

Owing to the rapid growth of various wireless communication services, considerable attention is being given to multiband transceivers, which are advantageous due to relatively low cost and small area occupation for mobile applications. In order for the multiband transceiver to provide seamless communications, it is essential to have a high-performance multiband bandpass filter (BPF) to avoid interference from different wireless bands which belong to the operation of the transceiver. In this regard, various research has been performed on, and several approaches have been developed for designing multiband BPFs. Especially, an enormous amount of work on dual BPF design has been presented based on the techniques of the loaded stub, frequency transformation, and coupling matrix. However, most of these studies only considered filters with specific passband responses [1–4]. In [5], a dual-conduction resonator was applied to fragment a wide passband into multiple passbands. However, it is challenging to achieve the desired frequency response of each passband in these techniques due to the non-negligible coupling of each resonator.

Typically, tri-band BPFs can be constructed by employing three sets of resonators with a common feed circuit [6]. However, the filter becomes bulky due to increased number of resonators. In order to miniaturize filter size, the researchers in [7] proposed a technique of assembling two resonators into one, while the authors in [8] presented a dual-band BPF using hybrid coded genetic algorithm technique. In [9], a technique for finding the coupling matrix of assembled resonators that can be used in dual and tri-band filters was proposed, and the researchers in [10] implemented the concept of degenerate modes in ring resonators to achieve a tri-band BPF. Also, a triple bandpass filter has been designed in [11] by the combination of stub loaded resonators and stepped impedance resonators. The center frequencies of this filter have been placed by adequately adjusting the length ratio, and impedance ratio of SLR and SIR, respectively. However, controlling these length and impedance ratio at the same time is very difficult. Utilizing the concept of [11], the authors in [12] designed the triple bandpass filter by using

Received 4 December 2017, Accepted 7 February 2018, Scheduled 14 February 2018
* Corresponding author: Jung-Dong Park (jdpark@dongguk.edu).
The authors are with the Division of Electronics and Electrical Engineering, Dongguk University, Seoul 04620, Republic of Korea.

asymmetric stepped impedance resonator with the concept of controlling impedance and length ratios of the asymmetric SIRs with only one step discontinuity. The implemented technique is quite attractive. However, it makes the circuit size so large to be implemented in portable devices.

Similarly, in [14], they designed a triple bandpass filter using tri-section stepped impedance resonators (TSSIRs) with zero-degree feedline and open stub. Frequency response at 2.4 GHz, 3.5 GHz, and 5.2 GHz can be precisely adjusted by adding the open stub line. In [15], a tri-bandpass filter is designed using the stub loaded resonator technique having main transmission line short ended with a centrally loaded open stub. Similarly, an advanced tri-bandpass filter is developed in [17] utilizing symmetrical tri-section stepped impedance resonators. However, the proposed structure has large circuit size and poor isolation. In all of these aforementioned designs, the resonant frequencies of all of the passbands were controlled by selecting the different electrical length and impedance ratios of the various resonators, which have led to massive size and limited applications.

In this paper, a compact tri-band BPF with low insertion loss (IL) and high selectivity is presented. The proposed filter utilizes two coupled stub-loaded dual-mode resonators (SLDMRs) instead of three sets of resonators. The passband frequencies are mainly determined by the entire length of the open loop and the length of the open stub. The two passband frequencies can be easily adjusted to the desired values by adequately adjusting the filter parameters predicted from the even- and odd-mode analysis while the odd-mode resonant frequency remains fixed, which provides advantageous design flexibility. The overall filter dimension is the same as that of the equivalent dual-passband filter as one set of resonators is implanted in the other. The structure of the filter is planar, compact, and simple to design. In addition, there is at least one transmission zero (TZ) on either edge of a passband, which manipulates the skirt selectivity with relatively small insertion-loss in the passbands. A method to control the position of the TZ's has been shown, and the corresponding coupling coefficient and an external quality factor of the filter is provided in detail. A prototype of the proposed filter is also implemented with derived design equations for the experimental verification.

2. ANALYSIS OF THE IMPLEMENTED RESONATOR

The implemented stub-loaded double mode resonator composed of the microstrip half wavelength resonator and an open stub is shown in Figure 1(a), where Y_1, L_1, Y_2, and L_2 represent the characteristic admittances and the lengths of the microstrip line and open stub, respectively. The open stub is shunted at the center of the line. Since the SLDMR is incorporated into the structure, we can examine it using the concept of odd-and even-mode analysis [1]. There is a null in the middle of the SLR for the excitation of the odd mode. The equivalent circuit of the odd mode is shown in Figure 1(b). Thus, the input admittance for the odd mode can be represented as:

$$Y_{in,odd} = \frac{Y_1}{j \tan\left(\frac{\theta_1}{2}\right)}, \tag{1}$$

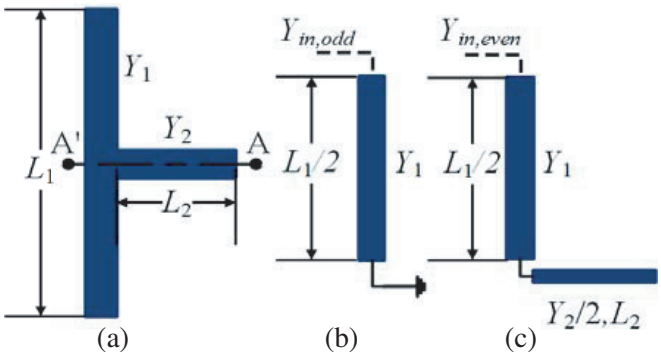

Figure 1. (a) Structure of the stub-loaded resonator. (b) Odd-mode equivalent circuit. (c) Even mode one.

where $\theta_1 = \beta L_1$ is the electrical length of the microstrip line with the length of L_1. At resonance, $Y_{in,odd} = 0$. Hence, the frequency of odd mode can be calculated by

$$f_{odd} = \frac{(2n+1)c}{2L_1\sqrt{\varepsilon_{eff}}}, \tag{2}$$

where $n = 0, 1, 2, 3, \ldots$, c is the speed of light in free space, and ε_{eff} is the effective dielectric constant of the substrate. The flow of current in the symmetrical plane of the SLR is zero at even-mode excitation, and so the equivalent even-mode circuit can be deduced as shown in Figure 1(c). The input admittance of the even mode can be calculated as:

$$Y_{in,even} = jY_1 \frac{2Y_1 \tan\left(\frac{\theta_1}{2}\right) + Y_2 \tan(\theta_2)}{2Y_1 - Y_2 \tan\left(\frac{\theta_1}{2}\right) j\tan(\theta_2)}, \tag{3}$$

where $\theta_2 = \beta L_2$ is the electrical length of the open stub with the length of L_2. Similarly, at the resonance frequency, $Y_{in,even} = 0$ and the frequency of the even mode can be calculated as:

$$\cot\left(\frac{\theta_1}{2}\right)\tan(\theta_2) = -\frac{2Y_1}{Y_2} \tag{4}$$

When we let Y_2 equal $2Y_1$, $\cot(\frac{\theta_1}{2})\tan(\theta_2) = -1$, thus the resonance condition can be deduced as:

$$\tan(\theta_2) = -\tan\left(\frac{\theta_1}{2}\right) => \theta_2 = n\pi - \tan^{-1}\left[\tan\left(\frac{\theta_1}{2}\right)\right], \tag{5}$$

$$\frac{\theta_1}{2} + \theta_2 = n\pi => \frac{L_1}{2} + L_2 = \frac{n\lambda_g}{2}, \tag{6}$$

where λ_g is the guided wavelength and the even mode resonant frequency can be calculated as:

$$f_{even} = \frac{nc}{(L_1 + 2L_2)\sqrt{\varepsilon_{eff}}}. \tag{7}$$

3. DESIGN AND RESULTS OF THE PROPOSED FILTER

Figure 2(a) shows the configuration of the BPF using two coupled SLDMRs combined with an internal open loop resonator. Compared with a conventional open-loop resonator [9], the proposed structure has an additional open stub embedded inside the open loop and another internal open loop resonator demonstrating that tri-band operation is attained without any further size increase. The passband frequencies are principally determined by the entire length of the open loop and the length of the open stub. The passband in the middle is determined by the intra-resonator coupling and the length of the internal resonator by controlling the gap (G_1). The substrate used for filter design is Rogers-RO5880TM having $\varepsilon_r = 2.2$ and a thickness of 0.7874 mm. Dimensions of the proposed tri-band filter are listed in Table 1.

Table 1. Dimensions (in Millimeters) of the proposed tri-band bandpass filter.

Symbol	Value	Symbol	Value	Symbol	Value	Symbol	Value	Symbol	Value	Symbol	Value
L_1	12.8 mm	L_2	18.7 mm	L_3	7.5 mm	L_4	8 mm	L_f	6 mm	d	1.4 mm
W_f	0.9 mm	W_s	1.5 mm	L_s	3 mm	G_1	0.25 mm	G_2&G_3	0.2 mm	W_1	1.2

Two SLDMRs combined with intra-resonator coupling between internal and external rings are utilized to achieve a tri-band BPF. The 3 dB fractional bandwidth (FBW) of three passbands are set as 10%, 5%, and 11% at their center frequency of 1.575, 2.40 and 3.45 GHz, respectively. The insertion loss method using the coupling coefficient $M_{i,j}$ and the external quality factor Q_{en} has been used to

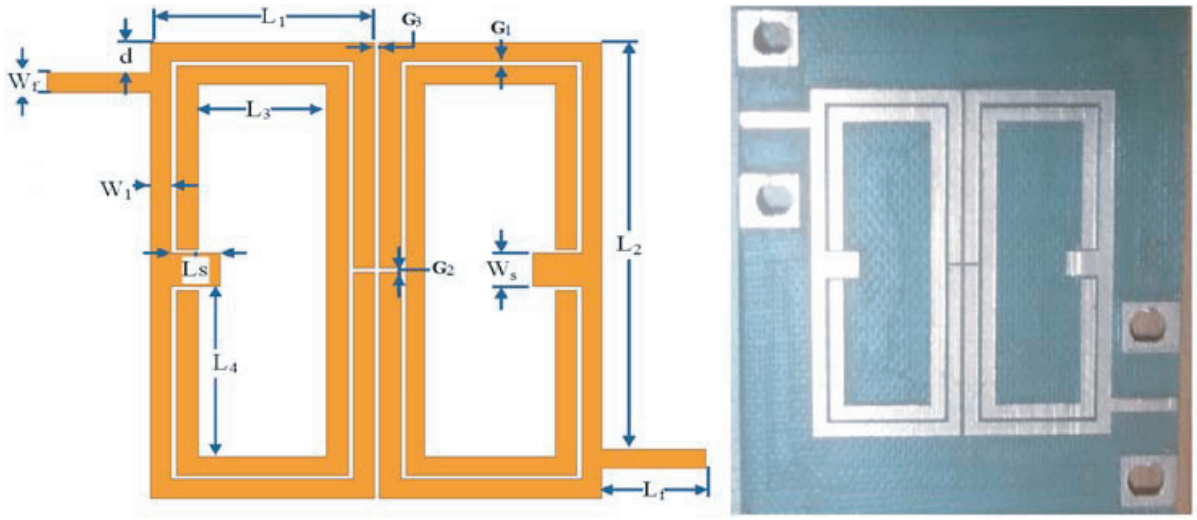

(a) (b)

Figure 2. (a) Proposed bandpass filter configuration. (b) Proposed bandpass filter prototype.

satisfy the specifications of all of the passbands. These parameters are respectively calculated using the following two equations [13]:

$$M_{i,i+1} = \frac{FBW}{\sqrt{g_i g_{i+1}}}, \tag{8}$$

$$Q_{en} = \frac{g_i g_{i+1}}{FBW}, \tag{9}$$

where g_i and g_{i+1} are the element values for the lowpass Chebyshev prototype having 2 dB ripples given as $g_0 = g_2 = 1$, $g_1 = 1.5296$ [18], and FBW is the 3 dB fractional bandwidth of the filter response.

The approximate synthesis of the element values for the filter can be calculated as [19]:

$$g_1 = \frac{2\sin\frac{\pi}{2n}}{\gamma}, \tag{10}$$

$$\gamma = \sinh\left(\frac{1}{n}\sinh^{-1}\frac{1}{\varepsilon_r}\right), \tag{11}$$

$$g_i g_{i-1} = \frac{4\sin\dfrac{(2i-1)\pi}{2n}\sin\dfrac{(2i-3)}{2n}}{\gamma^2 + \sin^2\dfrac{(i-1)\pi}{n}}, \quad i = 1, 2, \ldots, m, \tag{12}$$

where n is the number of the resonator sections, ε_r the effective relative permittivity of the substrate, and $m = n/2$.

Figure 3(a) shows that by varying the stub length (L_s), the fundamental even-mode resonance frequency can be shifted to the desired choice whereas the fundamental odd-mode resonant frequency is conserved. It is seen that by increasing stub length $L_s = 2$ mm to $L_s = 9$ mm, the corresponding upper passband frequency is shifting from 2.8 GHz to 3.6 GHz, respectively. Also, it is advantageous that the upper TZ can be controlled in the same manner just by changing the stub length as validated from Figure 3(a). All other passbands and TZ's are conserved at their center frequency while changing the stub length.

Figure 3(b) shows the simulated reflection coefficient and IL of the proposed filter. The three passbands are centered at 1.575, 2.4, and 3.45 GHz, corresponding the modern GNSS, WLAN, and WiMAX frequency bands. The frequency response is shown in Figure 3(b) also confirms the analytical results derived in Section 2. There also exist two TZ's on each side of the passband, which significantly isolates one passband from another.

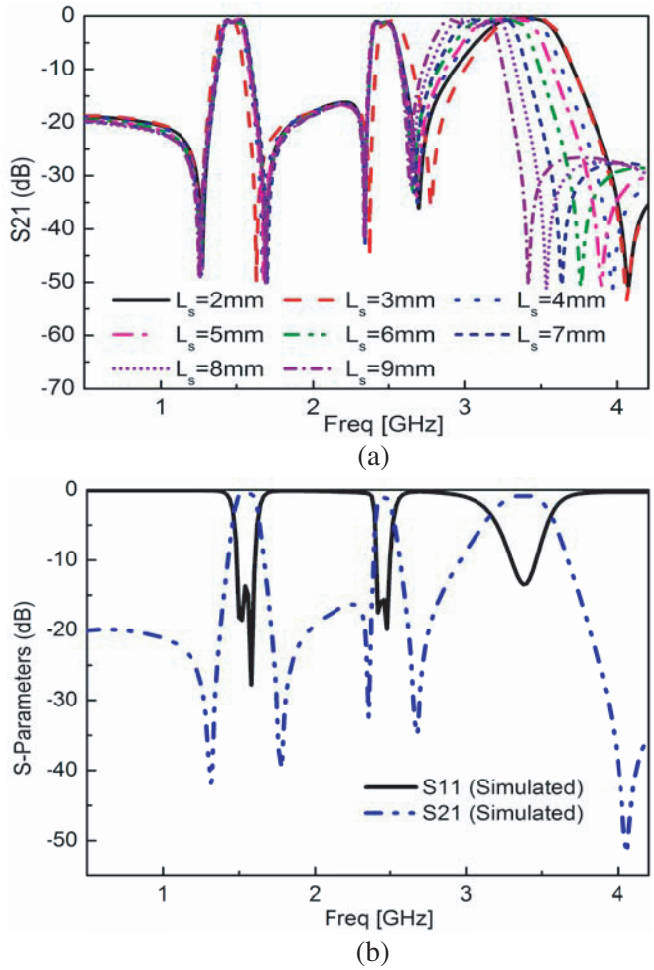

Figure 3. (a) Variation in the even mode resonance frequencies by varying the geometrical parameter (L_s) of the proposed tri-band bandpass filter predicted from the S21 plot. (b) Simulated frequency response of the proposed tri-band bandpass filter.

The geometrical parameter d determines the placement of the TZ's on either side of the passbands according to the desired frequency in the vicinity of the passband. This behavior of the filter is plotted and shown in Figure 4, which apparently reveals that each TZ can be adjusted accordingly by changing the parameter d while conserving the center frequencies of the passbands. This behavior of the filter makes them superior to another reported state of the art filters where the TZ's can be changed only by altering the center frequency of the passband. Also, the geometrical parameter d affects the external quality factor of the passbands as shown in Figure 5, calculated from the method provided in [11]. It is clear from Figure 5 that the effect is more dominant on Band-2 as compared to Band-1 and Band-3. It is also noteworthy that the external quality factor of all the passbands also slightly varies by changing the parameter d which in turn change the fractional bandwidth and the corresponding element values for the lowpass Chebyshev prototype. This is the reason that we can observe the modification of the passband ripple by changing d that is evident from Figure 4.

The intra-resonator coupling causes another passband at 2.4 GHz which depends on the geometrical parameter 'G_1'. By increasing G_1 the intra-resonator coupling decreases and at $G_1 = 1.2$ mm this coupling almost vanishes, and there is no passband anymore as shown in Figure 6. So, we have usefully utilized this intra-resonator coupling by optimizing the parameter G_1 in order to meet our requirements. The response of the proposed filter by varying the geometrical parameter G_1 having all other design parameters fixed is shown in Figure 6. The response clearly reveals that how the central passband is

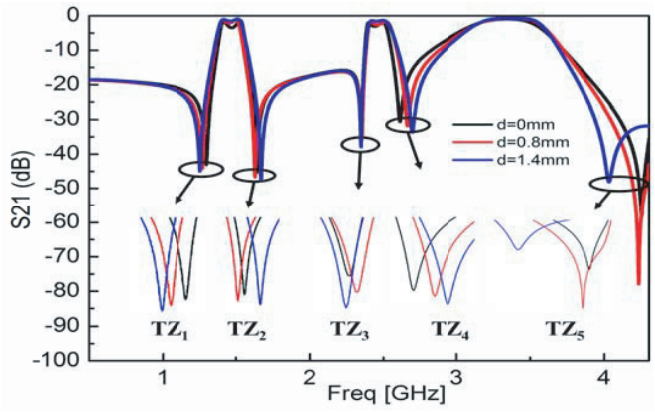

Figure 4. Shifting of transmission zeros (TZ's) by changing the geometrical parameter 'd'.

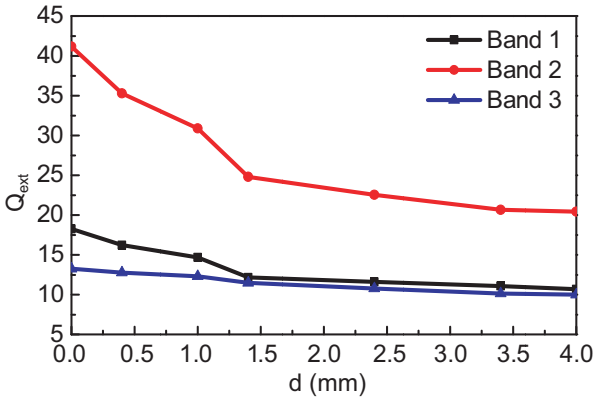

Figure 5. Effect of geometrical parameter 'd' on external quality factor 'Q_{ext}' of the proposed triple bandpass filter.

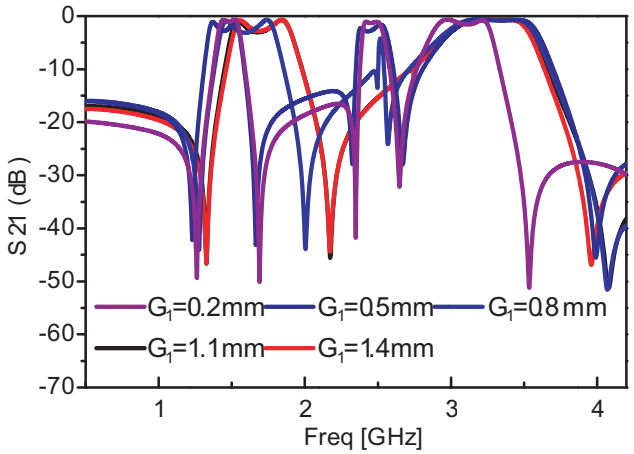

Figure 6. Effect of geometrical parameter 'G_1' on the frequency response of the proposed triple bandpass filter.

generated by analyzing the intra-resonator coupling within the embedded resonators.

The analysis of the coupling and external quality factor of the filter was carried out and showed that the parameter 'G_3' was able to control inter-resonator coupling. This inter-resonator coupling coefficient, k and external quality factor, Q_e, can be calculated from full wave simulated transmitted coefficients given by [11] as

$$k = \frac{f_h^2 - f_l^2}{f_h^2 + f_l^2}, \tag{13}$$

$$Q_e = \frac{\omega_0}{\Delta\omega_{(3\,\mathrm{dB})}}, \tag{14}$$

where f_l and f_h represent the lower and higher frequencies of the two resonant modes; ω_0 accounts for the resonant frequency; $\Delta\omega_{(3\,\mathrm{dB})}$ is the 3 dB bandwidth of the resonator centered with ω_0.

The coupling coefficient k and external quality factor Q_e of this filter are dependent on parameter G_3 as shown in Figure 7. Also, the parameter G_3 determines the bandwidth of all the passbands as its variation causes the change in the external quality factor of the proposed filter as predicted from Figure 7.

For the designed filter, the first passband is centered at 1.575 GHz for modern GNSS; it has an IL of 0.739 dB, and the reflection coefficient is better than −20 dB. Two TZ's can be observed adjacent

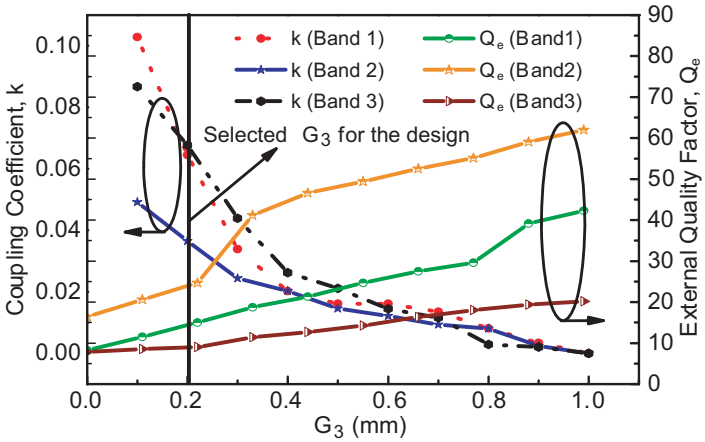

Figure 7. Coupling coefficient 'k' and external quality factor 'Q_e' vs. parameter 'G_3' of the proposed filter.

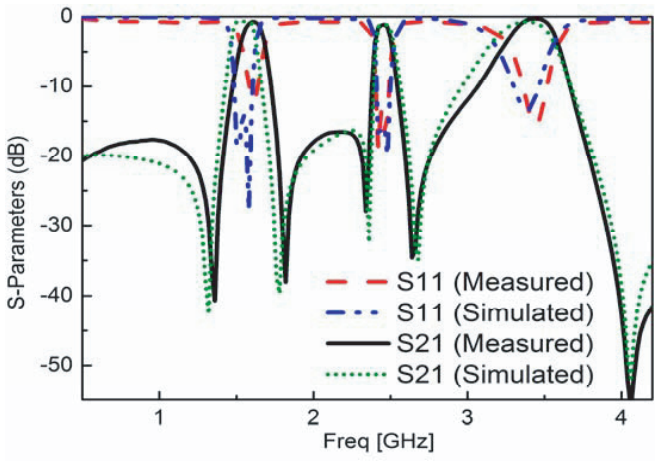

Figure 8. Simulated and measured results of the proposed filter.

to the passband edges at 1.31 and 1.76 GHz, which significantly improve the skirt selectivity. The bandwidth is almost 237 MHz, which covers the whole frequency range of the GNSS system, including GPS, GLONASS, Galileo, and Beidou. The second passband is positioned at 2.40 GHz for the WLAN system. The bandwidth is around 180 MHz with the lowest measured IL observed of 1.10 dB, and the reflection coefficient in the passband is better than 18 dB. Two TZ's are generated at 2.34 and 2.66 GHz, which are in the vicinity of the passband edges that considerably improve the roll-off characteristics, as shown in Figure 8. The third passband has a center frequency of 3.45 GHz, which is in the middle of the WiMAX band with a minimum IL of 0.45 dB, and the reflection coefficient within the desired band is better than 15 dB. The TZ observed in the upper stopband is at 3.94 GHz and the one placed at the lower stopband is at 2.66 GHz.

4. PROTOTYPE AND MEASUREMENTS OF THE FILTER

The 3D EM simulation and S-parameter measurements were accomplished with an Ansoft HFSS and a Keysight N5224A VNA, respectively. Figure 8 compares the simulated and measured responses of the BPF. The passbands of the proposed filter were located at 1.575, 2.4, and 3.45 GHz. The bandwidths were 237, 179, and 192 MHz, which covered the modern GNSS, WiFi, and WiMAX systems, respectively. The minimum ILs including the SMA connector was 0.74, 1.14, and 0.30 dB, respectively. Five TZ's

were generated at 1.31, 1.76, 2.34, 2.66, and 3.94 GHz, resulting in high isolation between each band. The corresponding BPF implemented on the Rogers-RO5880TM substrate is shown in Figure 2(b).

The comparisons between the proposed, designed filter and other recently reported state-of-the-art tri-band BPF designs are listed in Table 2. The proposed BPF possesses the advantages of low IL, maximum Tx-zeros, and compact size.

Table 2. Comparisons of the filters with other reported tri-band filters. (λ_0 is the free-space wavelength at the center of the first passband).

Source	1st/2nd/3rd Passband (GHz)	$\|S_{11}\|$ (dB)	$\|S_{21}\|$ (dB)	Circuit Size (mm^2) ($\lambda_0 \times \lambda_0$)	Max. Tx-Zeros
Ref. [2]	2.45/3.5/5.25	> 13	0.9/1.7/2.1	32×39.5 (0.93×1.14)	N/A
Ref. [3]	1.4/2.4/3.5	> 15	1.7/1.8/2.5	39.9×20.4 (0.72×0.36)	Three
Ref. [4]	2.5/3.5/5.8	17/13/15.1	0.8/2.3/2.4	28×48 (0.48×0.64)	Two
Ref. [10]	2.3/4.7/7.21	15/23/18	1.7/0.9/0.7	172×172 (5.6×5.6)	Five
Ref. [11]	1.575/2.4/3.45	9/18.9/13.5	1.6/1.5/2.3	49.7×56.2 (0.72×0.82)	Five
Ref. [12]	1.8/3.5/5.2	5.0/24/14	1.2/1.8/2	113.4×1.9 (1.89×0.03)	Two
Ref. [13]	1.35/1.44/1.60	12/15/22	0.8/1.4/0.5	43×42.2 (0.76×0.75)	Two
Ref. [14]	2.40/3.50/5.25	30/22/15	1.2/1.8/2.2	31×60.7 (0.57×0.86)	Three
Ref. [15]	1.95/3.46/5.25	N/A	1.1/1.5/1.5	35×35 (0.82×0.82)	Five
Ref. [16]	1.8/2.7/3.3–4.8	14/13/9	2.2/2.1/1.3	35.5×36.3 (0.82×0.83)	Four
Ref. [17]	1.0/2.4/3.6	15/30/17	2.0/1.9/1.7	40×40 (0.71×0.71)	N/A
This Work	1.575/2.4/3.45	18/22.3/17	0.7/1.14/0.3	31×38 (0.44×0.56)	Five

5. CONCLUSIONS

Based on SLDMR analysis, a compact tri-band BPF utilizing two coupled resonators with enhanced skirt selectivity in the vicinity of the passband having low insertion loss is presented. The passband frequencies can be independently adjusted to desired values by controlling the corresponding resonator dimensions. Five transmission zeros (TZ's) were realized, resulting in high selectivity of the passbands. The analysis has also been carried out on coupling coefficient and external quality factor. Also, the effects of the controlling geometrical parameters are discussed in detail. The proposed tri-band bandpass filter has been fabricated, and the calculations and simulations correspond well with the measured results. The multi-band operation, compact size, and planar structure of the proposed filter make it attractive for the use in portable wireless communication systems.

ACKNOWLEDGMENT

This work was supported by the Korea Institute of Energy Technology Evaluation and Planning (KETEP) and the Ministry of Trade, Industry & Energy (MOTIE) of the Republic of Korea (No. 20174030201520).

REFERENCES

1. Zhang, X. Y., J. X. Chen, and Q. Xue, "Dual-band bandpass filters using stub-loaded resonators," *IEEE Microwave and Wireless Components Letters*, Vol. 17, 583–585, 2007.
2. Lai, X., C. H. Liang, H. Di, and B. Wu, "Design of tri-band filter based on stub loaded resonator and DGS resonator," *IEEE Microwave and Wireless Components Letters*, Vol. 20, 265–267, 2010.

3. Lan, S. W., M. H. Weng, and S. J. Chang, "A tri-band bandpass filter with wide stopband using symmetric stub-loaded resonators," *IEEE Microwave and Wireless Components Letters*, Vol. 25, 19–21, 2015.
4. Wei, F., Y. J. Guo, P. Y. Qin, and X. W. Shi, "Compact balanced dual- and tri-band bandpass filters based on stub loaded resonators," *IEEE Microwave and Wireless Components Letters*, Vol. 25, 76–78, 2015.
5. Ma, D., Z. Y. Xiao, L. Xiang, X. Wu, C. Huang, and X. Kou, "Compact dual-band bandpass filter using folded SIR with two stubs for WLAN," *Progress In Electromagnetics Research*, Vol. 117, 357–364, 2011.
6. Lee, C. H., C. G. Hsu, and H. K. Jhuang, "Design of a new tri-band microstrip BPF using combined quarter-wavelength SIRs," *IEEE Microwave and Wireless Components Letters*, Vol. 16, 594–596, 2006.
7. Chen, F. C. and Q. X. Chu, "Design of compact tri-band bandpass filters using assembled resonators," *IEEE Transactions on Microwave Theory and Techniques*, Vol. 57, 165–171, 2009.
8. Lai, M. I. and S. K. Jeng, "Compact microstrip dual-band bandpass filters design using genetic-algorithm techniques," *IEEE Transactions on Microwave Theory and Techniques*, Vol. 54, 160–168, 2006.
9. Mokhtar, M., J. Bornemann, K. Rambabu, and S. Amari, "Coupling matrix design of dual and triple passband filters," *IEEE Transactions on Microwave Theory and Techniques*, Vol. 54, 3940–3946, 2006.
10. Luo, S., L. Zhu, and S. Sun, "Compact dual-mode triple-band bandpass filters using three pairs of degenerate modes in a ring resonator," *IEEE Transactions on Microwave Theory and Techniques*, Vol. 59, 1222–1229, 2011.
11. Chen, W. Y., M. H. Weng, and S. J. Chang, "A new tri-band bandpass filter based on stub-loaded step-impedance resonator," *IEEE Microwave and Wireless Components Letters*, Vol. 22, 179–181, 2012.
12. Chen, W. Y., S. J. Chang, M. H. Weng, Y. H. Su, and H. Kuan, "Simple method to design a tri-band bandpass filter using asymmetric SIRs for GSM, WiMAX and WLAN applications," *Microwave and Optical Technology Letters*, Vol. 53, 1573–1576, 2011.
13. Cao, L. and L. Yin, "Novel tri-band bandpass filter with high selectivity," *Progress In Electromagnetics Research Letters*, Vol. 51, 127–133, 2015.
14. Liu, B. and Y. Zhao, "Compact tri-band bandpass filter for WLAN and WiMAX using tri-section stepped-impedance resonators," *Progress In Electromagnetics Research Letters*, Vol. 45, 39–44, 2014.
15. Zhang, X. Y., L. Gao, Z. Y. Cai, and X. L. Zhao, "Novel tri-band bandpass filter using stub-loaded short-ended resonator," *Progress In Electromagnetics Research Letters*, Vol. 40, 81–92, 2013.
16. Chen, W. Y., M. H. Weng, S. J. Chang, H. Kuan, and Y. H. Su, "A new tri-band bandpass filter for GSM, WiMAX and ultra-wideband responses by using asymmetric stepped impedance resonators," *Progress In Electromagnetics Research*, Vol. 124, 365–381, 2012.
17. Chu, Q. X. and X. M. Lin, "Advanced triple-band bandpass filter using tri-section SIR," *Electronics Letters*, Vol. 44, 295–296, 2008.
18. Matthaei, G. L., L. Young, and E. M. T. Jones, "Couple strip transmission line filter sections," *Microwave Filters, Impedance-Matching Networks and Coupling Structures*, 217–228, Artech House, Norwood, MA, 1980.
19. Hong, J. S. G. and M. J. Lancaster, *Microstrip Filters for RF/Microwave Applications*, Vol. 167, John Wiley & Sons, 2004.